UC Davis
UC Davis Previously Published Works

Title

α1C S1928 Phosphorylation of CaV1.2 Channel Controls Vascular Reactivity and Blood Pressure.

Permalink

https://escholarship.org/uc/item/81c4m2j1

Journal

Journal of the American Heart Association, 13(20)

ISSN

2047-9980

Authors

Flores-Tamez, Victor A
Martín-Aragón Baudel, Miguel
Hong, Junyoung
et al.

Publication Date

2024-10-15

DOI

10.1161/jaha.124.035375

Peer reviewed

eScholarship.org Powered by the California Digital Library
University of California

Journal of the American Heart Association

ORIGINAL RESEARCH

$\alpha 1_C$ S1928 Phosphorylation of $Ca_V1.2$ Channel Controls Vascular Reactivity and Blood Pressure

Victor A. Flores-Tamez, PhD; Miguel Martín-Aragón Baudel, PhD; Junyoung Hong, PhD; Jade L. Taylor, PhD; Lu Ren, PhD; Thanhmai Le, BS; Arsalan U. Syed, PhD; Yumna Moustafa, BS; Navid Singhrao, PhD; Wendy R. Lemus-Martinez, BS; Gopireddy R. Reddy, PhD; Victoria Ramer, BS; Kwun Nok Mimi Man, PhD; Peter Bartels, PhD; Ye Chen-Izu, PhD; Chao-Yin Chen, PhD; Sergi Simo, PhD; Eamonn J. Dickson, PhD; Stefano Morotti, PhD; Eleonora Grandi, PhD; L. Fernando Santana, PhD; Johannes W. Hell, PhD; Mary C. Horne, PhD; Madeline Nieves-Cintrón, PhD; Manuel F. Navedo, PhD

BACKGROUND: Increased vascular $Ca_V1.2$ channel function causes enhanced arterial tone during hypertension. This is mediated by elevations in angiotensin II/protein kinase C signaling. Yet, the mechanisms underlying these changes are unclear. We hypothesize that $\alpha 1_C$ phosphorylation at serine 1928 (S1928) is a key event mediating increased $Ca_V1.2$ channel function and vascular reactivity during angiotensin II signaling and hypertension.

METHODS AND RESULTS: The hypothesis was examined in freshly isolated mesenteric arteries and arterial myocytes from control and angiotensin II-infused mice. Specific techniques include superresolution imaging, proximity ligation assay, patch-clamp electrophysiology, Ca^{2+} imaging, pressure myography, laser speckle imaging, and blood pressure telemetry. Hierarchical "nested" and appropriate parametric or nonparametric *t* test and ANOVAs were used to assess statistical differences. We found that angiotensin II redistributed the $Ca_V1.2$ pore-forming $\alpha 1_C$ subunit into larger clusters. This was correlated with elevated $Ca_V1.2$ channel activity and cooperativity, global intracellular Ca^{2+} and contraction of arterial myocytes, enhanced myogenic tone, and altered blood flow in wild-type mice. These angiotensin II-induced changes were prevented/ameliorated in cells/arteries from S1928 mutated to alanine knockin mice, which contain a negative modulation of the $\alpha 1_C$ S1928 phosphorylation site. In angiotensin II-induced hypertension, increased $\alpha 1_C$ clustering, $Ca_V1.2$ activity and cooperativity, myogenic tone, and blood pressure in wild-type cells/tissue/mice were averted/reduced in S1928 mutated to alanine samples.

CONCLUSIONS: Results suggest an essential role for $\alpha 1_C$ S1928 phosphorylation in regulating channel distribution, activity and gating modality, and vascular function during angiotensin II signaling and hypertension. Phosphorylation of this single vascular $\alpha 1_C$ amino acid could be a risk factor for hypertension that may be targeted for therapeutic intervention.

Key Words: cardiovascular ■ clustering ■ cooperativity ■ diabetes ■ hypertension

See Editorial by Jensen.

Correspondence to: Madeline Nieves-Cintrón, PhD and Manuel F. Navedo, PhD (Lead Contact), Department of Pharmacology, University of California Davis, One Shields Avenue, MED: PHARM Tupper 2219A, Davis, CA 95616. Email: mcnieves@ucdavis.edu and mfnavedo@ucdavis.edu

This article was sent to Barry London, MD, PhD, Senior Guest Editor, for review by expert referees, editorial decision, and final disposition.

Supplemental Material is available at https://www.ahajournals.org/doi/suppl/10.1161/JAHA.124.035375

For Sources of Funding and Disclosures, see page 15.

© 2024 The Author(s). Published on behalf of the American Heart Association, Inc., by Wiley. This is an open access article under the terms of the Creative Commons Attribution-NonCommercial-NoDerivs License, which permits use and distribution in any medium, provided the original work is properly cited, the use is non-commercial and no modifications or adaptations are made.

JAHA is available at: www.ahajournals.org/journal/jaha

CLINICAL PERSPECTIVE

What Is New?

- Phosphorylation of $\alpha 1_C$ at serine 1928 (S1928) controls $Ca_V1.2$ channels spatiotemporal remodeling during activation of angiotensin II signaling and hypertension.
- Phosphorylation of $\alpha 1_C$ at S1928 underlies increased arterial myocyte intracellular calcium, vascular reactivity, and blood pressure during angiotensin II signaling and hypertension.

What Are the Clinical Implications?

- Phosphorylation of $\alpha 1_C$ at S1928 may be a rheostat of vascular function in health and disease.
- Increased phosphorylation of $\alpha 1_C$ at S1928 may be a risk factor underlying vascular complications during hypertension.
- Results may help develop therapeutics with single amino acid accuracy to reduce $\alpha 1_C$ S1928 phosphorylation, which may ameliorate hypertension-related vascular complications.

Nonstandard Abbreviations and Acronyms

$[Ca^{2+}]_i$	intracellular Ca^{2+} concentration
Ang II	angiotensin II
BPH	blood pressure high
nPo	number of channels X open probability
PKA	protein kinase A
PKC	protein kinase C
PLA	proximity ligation assay
pS1928	S1928 phosphorylation
S1928	serine1928
WT	wild-type

L-type $Ca_V1.2$ channels are essential for excitation-contraction coupling and gene expression in many cells,[1] including arterial myocytes.[2] Ca^{2+} influx through single or clustered $Ca_V1.2$ exerts a major regulatory influence on vascular reactivity, blood flow, and blood pressure (BP) in health and diseases such as hypertension.[3–5] Indeed, increased vascular $Ca_V1.2$ activity is a major driver of arterial remodeling and elevated myogenic tone during hypertension.[3,5–8] Hypertension is also characterized by enhanced angiotensin II (Ang II) signaling,[9–11] which acting via the angiotensin type 1 receptor/G_q/ PKCα (protein kinase Cα) axis stimulates vascular $Ca_V1.2$ activity.[3,6,7,12–14] Yet, the precise $Ca_V1.2$ activating mechanism, the impact on vascular reactivity, and the link to hypertension are unknown. Addressing these issues is important as it provides new insights into how vascular $Ca_V1.2$ and arterial function are regulated in hypertension and may identify new therapeutic targets.

$Ca_V1.2$ channels are heterotrimeric proteins made of a pore-forming $\alpha 1_C$ (Figure S1A) and accessory β and $\alpha_2\delta$ subunits.[1,2] The $\alpha 1_C$ subunit is the target of many signaling pathways, such as PKA (protein kinase A) and PKC.[1,2] The regulation of native $Ca_V1.2$ channels by PKA has been attributed to various mechanisms depending on the tissue. Accordingly, PKA regulation of the cardiac $Ca_V1.2$ is mediated by the small GTPase Rad.[15,16] In stark contrast, direct phosphorylation of the $\alpha 1_C$ subunit at serine 1928 (S1928; Figure S1A) is required for the regulation of $Ca_V1.2$ in neurons and arterial myocytes.[17–21] Conversely, PKC regulation of $Ca_V1.2$ channels has been thought to be mediated by phosphorylation of the pore-forming $\alpha 1_C$.[22,23] Biochemical data in heterologous expression systems identified $\alpha 1_C$ S1928 as a potential PKC phosphorylation site.[24,25] This observation led us to hypothesize that phosphorylation of the $\alpha 1_C$ subunit at S1928 is essential to regulate $Ca_V1.2$ channel function in arterial myocytes in response to Ang II signaling and hypertension. We also proposed that S1928 phosphorylation (pS1928) is necessary for the modulation of myogenic tone, blood flow, and blood pressure. Considering that the α1c sequence shows >95% identity between rodent and human sequences (Figure S1B)[26] and that the S1928 residue is 100% identical between species (Figure S1C),[26] as well as recent studies showing a key role for pS1928 in regulating $Ca_V1.2$ channel activity and vascular function to a similar extent in both rodents and humans during diabetes,[20,27,28] we submit that pS1928 may also be involved in mediating alterations in $Ca_V1.2$ activity and vascular function in human hypertension.

To test our hypotheses, we employed a multiscale approach involving superresolution microscopy, proximity ligation assay (PLA), patch-clamp electrophysiology, Ca^{2+} imaging, pressure myography, laser speckle imaging, BP telemetry, and different animal models of hypertension such as Ang II-induced hypertensive mice and genetically induced BP high (BPH) mice. We took advantage of a knockin mouse with S1928 mutated to alanine to prevent pS1928 (ie, S1928A mouse[29]). Results implicate pS1928 as a key factor mediating $Ca_V1.2$ nanostructural and functional changes leading to vascular complications during enhanced Ang II signaling and hypertension.

METHODS

Data Availability Statement

All data are included in the article, and detailed methodology, (Table S1), (Figures S1 through S12), full unedited blots, and source Matlab codes are included in Data S1.

Mouse Study Approval

Given the well-known sex-dependent differences in Ang II-induced hypertension,[30] male wild-type (WT) C57BL/6J and S1928A[29] mice and male BP normal (BPN) and BPH mice were used to properly power experiments to resolve statistical differences between data sets. To assess potential sex differences, a set of properly powered experiments were done using female mice/samples, although this was not a primary goal of the study. All studies conform with the US National Institutes of Health *Guide for the Care and Use of Laboratory Animals* and were carried out in strict accordance with the protocols and guidelines approved by the Institutional Animal Care and Use Committee of the University of California, Davis.

In Vivo Ang II Infusion

Chronic Ang II infusion was performed using minipumps subcutaneously implanted in WT and S1928A mice.[3,7]

Dissection of Mesenteric Arteries and Isolation of Arterial Myocytes

Mice were euthanized by a lethal intraperitoneal injection of sodium pentobarbital. Mesenteric arteries were isolated, and arterial myocytes were dissociated using enzymatic/mechanical dissociation.[31]

Electrophysiology

Whole-cell and cell-attached electrophysiology was performed in isolated mesenteric arterial myocytes using an Axopatch 200B amplifier. Data were analyzed using pClamp.[28]

Computational Modeling

Simulations were performed using an established mathematical model of membrane electrophysiology and Ca^{2+} cycling.[32,33]

Imaging of Cell Ca^{2+} and Contraction

Ca^{2+} imaging in mesenteric cells was performed using a spinning disk confocal microscope. The fluorescence signal was also used to calculate contractility.[28]

Superresolution and PLA

α_{1C} protein distribution and clustering were determined using a direct stochastic optical reconstruction microscopy superresolution microscope. PLA was used to define close association of α_{1C} subunits.[20,28]

Laser Speckle

Blood flow in anesthetized animals was measured using laser speckle imaging. Edge detection was used to calculate arterial diameter from the images.[27,28]

Pressure Myography

Myogenic/vascular tone was calculated in pressurized mesenteric arteries.[20,27,28]

Blood Pressure and Echocardiography

BP was measured in freely moving mice using DSI telemetry.[34] Echocardiography was performed in anesthetized mice using a Vevo 2100 system.

Statistical Analysis

Data were analyzed using GraphPad Prism v10 or R Studio software and expressed as mean±SEM. The Shapiro–Wilk normality test was used to assess whether a data set deviated significantly from a normal (eg, Gaussian) distribution. The comparisons between groups were performed using hierarchical "nested" analyses to account for the number of mice and replicates,[35] with appropriate *t* test, 1-way ANOVA, 2-way ANOVA, and 3-way ANOVA with Bonferroni post hoc test. Parametric or nonparametric *t* tests and ANOVAs were applied when nested analyses were not implemented. Unless otherwise indicated, $P<0.05$ was considered statistically significant.

RESULTS

All experiments were performed using freshly isolated mouse mesenteric arteries and arterial myocytes (ie, immediate use after isolation/dissociation). The rationale for this is that mesenteric arteries and arterial myocytes play a key role in regulating BP, and their use immediately after isolation/dissociation may better reflect the native environment.

Ang II Increases Vascular $Ca_V1.2$ Function Via pS1928

Acute Ang II exposure has been shown to increase $Ca_V1.2$ channel activity in arterial myocytes.[3,7,36,37] Using whole-cell patch clamp with barium as the charge carrier and a single voltage step from −70 to +10 mV (maximal current),[18,20,27,28,38] we confirmed that Ang II exposure increased $Ca_V1.2$ current density (whole-cell barium current) in WT arterial myocytes (Figure 1A). In stark contrast, Ang II failed to augment whole-cell barium current in arterial myocytes from a genetically modified mouse in which the $\alpha 1_C$ serine 1928 position was mutated to alanine to prevent its phosphorylation (S1928A mouse[29]; Figure 1A).

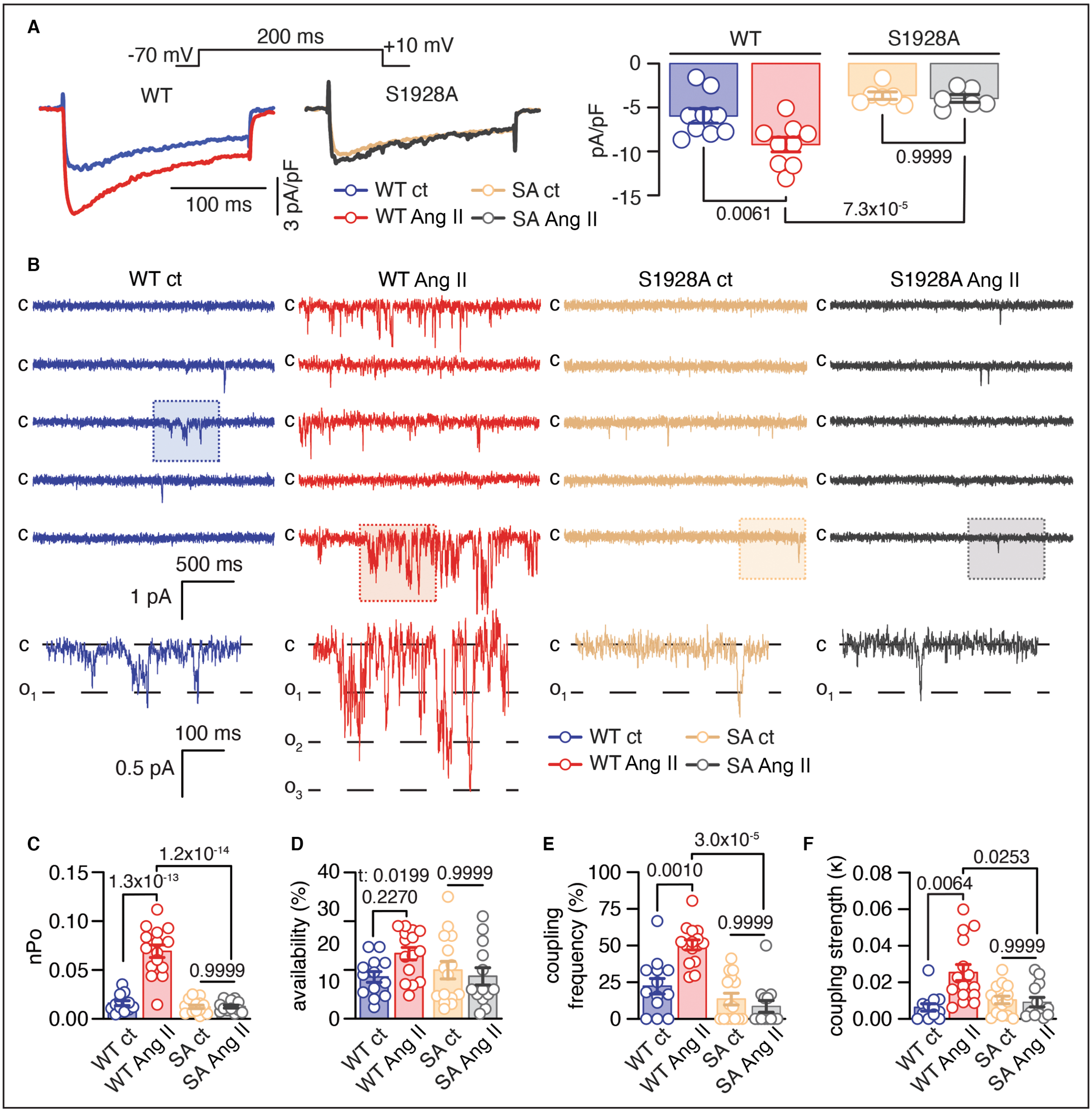

Figure 1. pS1928 controls $Ca_V1.2$ biophysical properties upon Ang II exposure.
A, Representative nifedipine-sensitive Ba^{2+} currents (I_{Ba}) elicited by a single voltage step from −70 mV to +10 mV recorded from WT and SA arterial myocytes under control conditions and after exposure to 100 nmol/L Ang II. The right-side panel shows summary scatter plots (WT: n=9 cells from 4 mice; SA ct: n=6 cells from 3 mice). Significance was assessed with nested 2-way ANOVA with Bonferroni post hoc test (*P*=0.0473). **B**, Exemplary single-channel traces obtained in cell-attached mode using a single voltage step from −80 mV to −30 mV recorded from WT and S1928A arterial myocytes under control conditions and after exposure to 100 nmol/L Ang II. Ca^{2+} was used as the charge carrier to visualize Ca^{2+}-dependent $Ca_V1.2$ cooperative events. Sections of the traces in the boxes are magnified below for a detailed appreciation of openings and cooperative events. The baseline level is highlighted by a (c) and unitary levels by (o_n). Summary data of (**C**) channel activity (nPo), (**D**) channel availability, (**E**) coupling frequency, and (**F**) coupling strength (κ) (WT ct: n=13 cells from 7 mice; WT Ang II: n=15 cells from 6 mice; SA ct: n=15 cells from 5 mice; SA Ang II: n=13 cells from 5 mice). Significance was assessed with nested 2-way ANOVA with Bonferroni post hoc test ($P=1.9\times10^{-9}$ for 1C; *P*=0.0615 for **D**—significant change at *P*<0.1 and unpaired *t* test between WT ct and WT Ang II with *P*=0.0199 (t in graph); *P*=0.0016 for **E**; *P*=0.0132 for **F**). Data are mean±SEM. *P* values for relevant comparisons within each panel and supplemental material. Ang II indicates angiotensin II; ct, control conditions; nPO, number of channels X open probability; pS1928, serine 1928 phosphorylation; SA, serine 1928 mutated to alanine; and WT, wild type.

Accordingly, the Ang II-induced change in whole-cell barium current was 3.3±0.6 pA/pF in WT cells versus 0.3±0.2 pA/pF in S1928A cells (P=0.0028 with unpaired t test; Shapiro–Wilk normality test P =0.6173). Note that $\alpha 1_C$, and PKCα (Figure S2), as well as BKα, BKβ1, and K_V2.1 protein abundance in arterial lysates[20] and basal voltage dependency of activation and inactivation of Ca_V1.2 channels, are similar in WT and S1928A male arterial myocytes,[28] suggesting that changes in the expression of key proteins and Ca_V1.2 biophysical properties do not account for the Ang II effects. These results indicate that pS1928 is necessary for Ang II-induced potentiation of vascular whole-cell barium current in male arterial myocytes.

Activation of Ang II signaling has been shown to promote cooperative gating of vascular Ca_V1.2 channels.[3,6,7] To examine if pS1928 is important for this gating mode, cell-attached electrophysiology with Ca^{2+} as the charge carrier was done in freshly isolated WT and S1928A male arterial myocytes. Ang II significantly increased Ca_V1.2 channel nPo (ie, n is the number of channels and Po is the channel open probability; Figure 1B and 1C) and availability (ie, likelihood of at least one event per sweep; Figure 1B and 1D) in WT cells (nested t test between WT controls and WT Ang II). In addition, the frequency of Ca_V1.2 cooperative events (ie, number of traces showing openings with 2 or more channels; see insets in Figure 1B) and the coupling strength (ie, $\varkappa$, which was quantified using a Markov chain model[6,39]) were higher in WT cells after Ang II (Figure 1E and 1F). Conversely, Ang II failed to increase Ca_V1.2 channel nPo, availability, coupling frequency, or coupling strength in S1928A cells (Figure 1B through 1F). Results in control and Ang II-treated S1928A male cells were comparable to WT male controls. Overall, these results suggest that pS1928 is necessary for Ang II to increase Ca_V1.2 channel activity and cooperative gating behavior.

Similar single-channel experiments performed in WT female arterial myocytes revealed no differences in nPo and coupling frequency but significant differences in availability and coupling strength compared with WT male cells (Figure S3A through S3E). Ang II increased coupling frequency, and trends toward higher values were found in nPo and availability properties but not coupling strength in female arterial myocytes (Figure S3A and S3F through S3I). These results suggest sex-dependent differences in basal conditions and mechanisms by which Ang II modulates vascular Ca_V1.2 channel activity and cooperative gating.

pS1928 Mediates Ang II-Induced Vascular $\alpha 1_C$ Clustering

The Ang II-induced elevations in Ca_V1.2 cooperative gating prompted us to examine if this was due to increased $\alpha 1_C$ clustering in the sarcolemma of arterial myocytes. For this, we performed superresolution imaging of $\alpha 1_C$ in freshly dissociated male mesenteric arterial myocytes (Figure 2A).[20,28] We used pair-correlation analysis to characterize the physical properties of $\alpha 1_C$ clusters and objectively quantify spatial scales of density fluctuations (Figure 2B).[40,41] This analysis is not influenced by the multiple appearances of a single fluorescent molecule detected multiple times across all frames before being irreversibly photobleached.[40,41] Data revealed a significant increase in cluster size (Figure 2C) and the estimated number of molecules per cluster ($N^{clusters}$; Figure 2E) but not cluster density (Figure 2D) in WT arterial myocytes after Ang II. Changes in $\alpha 1_C$ cluster size and $N^{clusters}$ were a direct consequence of pS1928, as cluster size (Figure 2C), cluster density (Figure 2D), and $N^{clusters}$ (Figure 2E) were similar in S1928A cells in control and Ang II conditions and comparable to WT control cells. Note that PKA inhibition does not prevent the increase in Ang II-induced $\alpha 1_C$ clustering properties (Figure S4A through S4E). Thus, PKA is not involved in the pathway triggering the $\alpha 1_C$ clustering in response to Ang II.

Intriguingly, superresolution experiments in female mesenteric arterial myocytes found an increase in basal $\alpha 1_C$ cluster size and density, but not $N^{clusters}$, compared with male mesenteric myocytes (Figure S55A and S5C through S5E). Moreover, Ang II did not elicit significant changes in $\alpha 1_C$ cluster size, cluster density, and $N^{clusters}$ in female WT and S1928A myocytes (Figure S4A, S4B, S4F through S4H). These results reveal sex-dependent differences in $\alpha 1_C$ clustering mechanisms at the basal and Ang II-stimulated levels.

The superresolution results in male arterial myocytes were confirmed using a modified PLA approach with an $\alpha 1_C$ monoclonal antibody labeled with the PLUS or MINUS probe that has been extensively validated to test $\alpha 1_C$ oligomerization/clustering (Figure 2F).[28,31] PLA showed that Ang II increased the number of $\alpha 1_C$ PLA puncta per cell area in WT male arterial myocytes but not WT cells pretreated with a broad PKC inhibitor or S1928A cells (Figure 2G through 2I). PKC inhibition in WT cells did not change the $\alpha 1_C$ PLA puncta per cell area compared with WT control and PLA puncta were never observed if 1 of the primary antibody probes was omitted (Figure 2G and 2I). These results suggest Ang II/PKC-dependent pS1928 increases $\alpha 1_C$ clustering in male arterial myocytes.

Ang II Increases Arterial Myocyte Ca^{2+} and Contractility Via pS1928

Ca_V1.2 cooperative gating amplifies Ca^{2+} influx into cells, accounting for ~50% of the total Ca^{2+} influx in arterial myocytes.[4,42] This is important because Ang II promotes this Ca_V1.2 gating modality, influencing

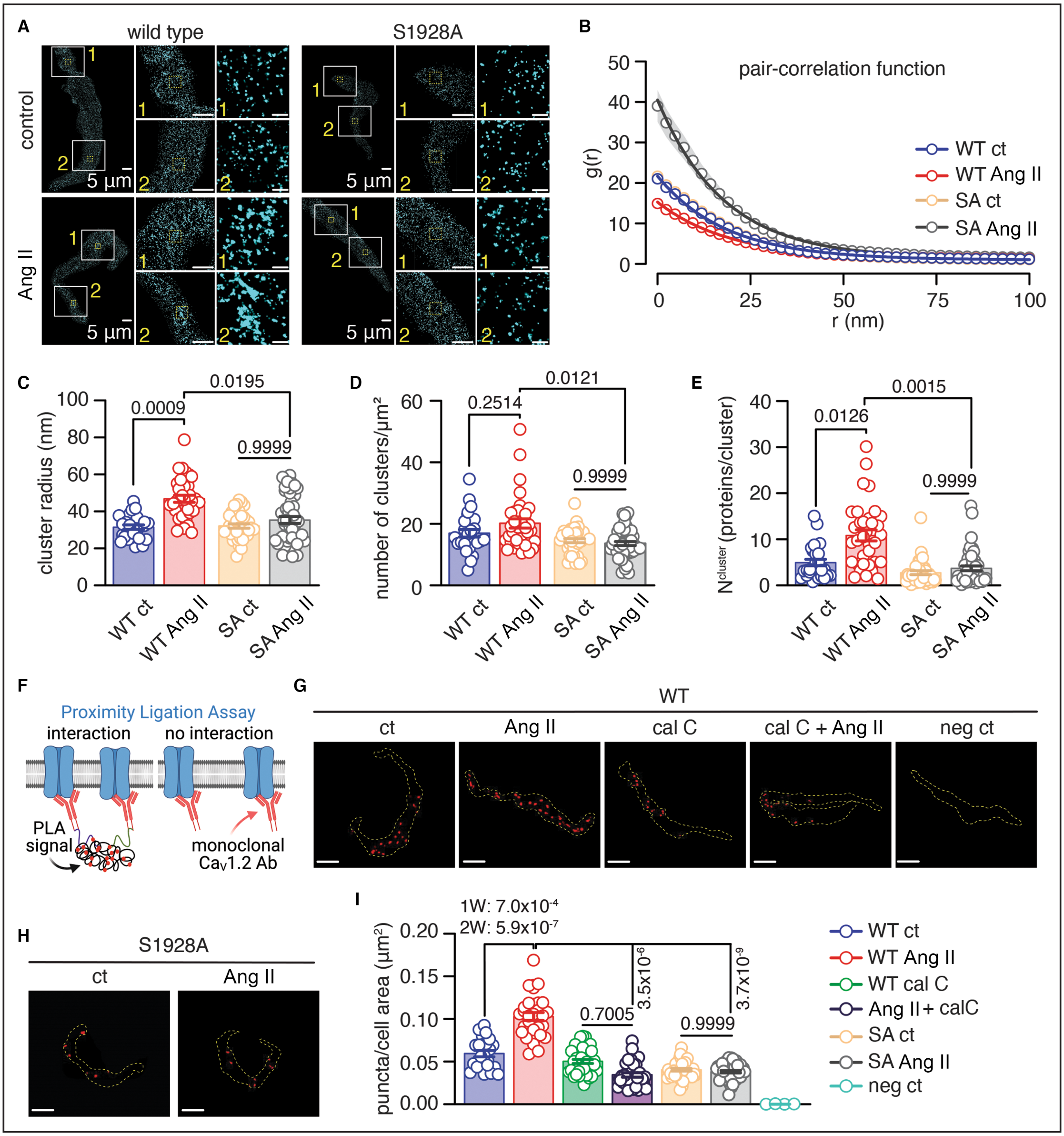

arterial myocyte Ca^{2+} and contractility. Thus, the role of pS1928 in modulating arterial myocyte excitability in response to Ang II signaling was initially investigated using an in silico model. We did this to prevent over-simplification and consider the complex cascade of ionic conductances that may be altered and influence cell electrophysiology and Ca^{2+} properties during Ang II signaling activation.[32,33] The model was fitted with experimental data showing Ang II-induced alterations in the activity of $Ca_V1.2$ channels, several K^+ channels, and transient receptor potential channels.[3,7,43–46] We also modeled the effect of preventing pS1928 (as in S1928A cells) upon Ang II to assess the role of pS1928 on arterial myocyte membrane potential and $[Ca^{2+}]_i$. The model predicted that Ang II could promote arterial myocyte membrane depolarization in WT and S1928A cells, but pS1928 was still necessary for elevating $[Ca^{2+}]_i$ in arterial myocytes (Figure 3A). To test this prediction, we first measured the membrane potential of WT and S1928A freshly isolated arterial myocytes upon Ang II using the perforated whole-cell patch-clamp.[28,31] Basal membrane potential was similar in WT (−56±2 mV) and

Figure 2. Ang II increased $\alpha1_C$ clustering requires pS1928.

A, Exemplary superresolution total internal reflection fluorescence images of WT and SA arterial myocytes labeled for $\alpha1_C$ with 2 magnified areas under control conditions and after exposure to 100 nmol/L Ang II (scale bars=5 μm→5 μm→200 nm). **B**, Plot of the calculated pair-correlation function (g(r)) of $\alpha1_C$ clusters in WT and SA arterial myocytes under control conditions and after 100 nmol/L Ang II exposure. Scatter plots of (**C**) $\alpha1_C$ cluster radius (nm), (**D**) $\alpha1_C$ cluster density (number of clusters/μm^2) and (**E**) estimated $\alpha1_C$ proteins per cluster ($N^{cluster}$) in WT and SA arterial myocytes under control conditions and after 100 nmol/Ls Ang II exposure (WT ct: n=27 cells from 7 mice; WT Ang II: n=34 cells from 7 mice; SA ct: n=38 cells from 5 mice; SA Ang II: n=50 cells from 7 mice). Significance was assessed with nested 2-way ANOVA with Bonferroni post hoc test (P=0.0268 for **C**; P=0.0676 for interaction and P=0.0108 for **D**; P=0.0342 for **E**). **F**, Cartoon of the modified PLA approach. Representative maximal projection images of PLA puncta for $\alpha1_C$-$\alpha1_C$ interactions in WT (**G**) and SA (**H**) male arterial myocytes under control conditions, after Ang II treatment or Ang II+cal C. The fifth image is a representative negative control image for PLA in which only 1 anti-$\alpha1_C$-tagged antibody was added to WT ct arterial myocytes. Dotted lines outline the cells. Scale bars=10 μm. **I**, Scatter plot of PLA $\alpha1_C$-$\alpha1_C$ puncta per cell area (μm^2) in WT ct, WT Ang II, WT+cal C, WT Ang II+cal C, SA ct, and SA Ang II arterial myocytes (WT ct: n=23 cells from 5 mice; WT Ang II: n=31 cells from 5 mice; WT+cal C: n=40 cells from 6 mice; WT Ang II+cal C: n=31 cells from 5 mice; SA ct: n=46 cells from 5 mice; SA Ang II: n=46 cells from 5 mice). WT arterial myocytes treated with only 1 of the PLA probes were used as negative control (neg ct; n=4 cells from 2 mice). Significance was assessed with nested 1-way ANOVA (1W) for WT comparisons or nested 2-way ANOVA (2W) for WT/SA comparisons with Bonferroni post hoc test ($P=4.1\times10^{-6}$ for WT comparisons; $P=1.3\times10^{-5}$ for WT/SA comparisons). Data are mean±SEM. P values for relevant comparisons within each panel and supplemental material. Ang II indicates angiotensin II; cal C, calphostin C; ct, control conditions; PLA, proximity ligation assay; pS1928, serine 1928 phosphorylation; SA, serine 1928 mutated to alanine; and WT, wild type.

S1928A (−57±2 mV) cells (Figure 3B and 3C). Ang II depolarized membrane potential to about the same magnitude in both cell types (−35±3 mV in WT and −32±3 mV in S1928A; Figure 3B and 3C). These results are consistent with the in silico prediction and suggest that Ang II effects on membrane potential in arterial myocytes are not reliant on pS1928.

To test the prediction that pS1928 is necessary for Ang II-induced elevations in $[Ca^{2+}]_i$, male arterial myocytes loaded with the Ca^{2+} indicator fluo 4-AM were used. This fluorescent signal was also used to track cell length and assess contractility (see Methods for details).[28] Data showed that Ang II increased peak $[Ca^{2+}]_i$ with a concomitant contraction in WT arterial myocytes (Figure 3D through F). WT cells pretreated with the $Ca_V1.2$ channel blocker nifedipine or the broad PKC inhibitor calphostin C did not show the Ang II-induced elevation in $[Ca^{2+}]_i$ and cell contraction, indicating that $Ca_V1.2$ channel activity and PKC are required for the Ang II effects. Moreover, Ang II failed to elevate $[Ca^{2+}]_i$ and induce contraction in S1928A cells. These results are consistent with the in silico model prediction and suggest that pS1928 is necessary for the Ang II-induced, PKC-dependent elevation of $[Ca^{2+}]_i$ leading to contraction of male arterial myocytes.

pS1928 Regulates Arterial Diameter and Blood Flow

We measured vascular tone ex vivo in response to Ang II in WT and S1928A mesenteric arteries to corroborate pS1928 physiological relevance. Mesenteric arteries from WT and S1928A male mice were freshly dissected and pressurized to 80 mm Hg. Basal myogenic tone (ie, pressure-induced constriction) was lower in S1928A mesenteric arteries compared with WT (Figure 4A and 4B). When exposed to Ang II, both WT and S1928A arteries constricted to about the same magnitude (Figure 4A and 4C). However, in the continuous presence of Ang II, WT arteries reached a new steady-state plateau level with higher vascular tone (ie, agonist-induced constriction) compared with S1928A arteries (Figure 4A and 4D). Similar Ang II-induced responses were observed in pressurized cerebral pial arteries (Figure S6A through S6D), suggesting conserved mechanisms in different vascular beds. These data indicate that Ang II-induced elevation in steady-state tone in male arteries requires pS1928.

To confirm the in vivo physiological significance of pS1928 upon Ang II signaling activation, arterial diameter and blood flow were measured in response to different Ang II concentrations in exposed mesenteric arteries of anesthetized WT and S1928A male mice using laser speckle imaging.[27,28,38] A solution containing vasodilatory drugs was used to promote maximal dilation to normalize arterial diameter and blood flow measurements. Under control conditions, basal tone was higher and corresponding blood flow was lower in mesenteric arteries of WT male mice compared with S1928A (Figure 4E, 4G, and 4H), consistent with the ex vivo basal tone data. Ang II induced a concentration-dependent decrease in arterial diameter and concomitant reduction in blood flow (ie, flux) in mesenteric arteries from WT and S1928A mice (Figure 4E and 4F). Peak constriction and corresponding flux were relatively similar at most points examined immediately after Ang II (Figure 4F, 4I, and 4J; Figure S6E and S6F). However, 5 minutes after Ang II, arteries from the S1928A mice showed larger diameter and flux compared with arteries from WT male mice (Figure 4E, 4F and 4I through 4L). The $Ca_V1.2$ channel blocker nifedipine prevented the Ang II effects on arterial diameter and flux (Figure 4I through L and Figure S6E and S6F). Altogether, these results suggest a key role for pS1928 and L-type Ca^{2+} channels in the in vivo regulation of male arterial diameter (and vascular tone) and blood flow upon Ang II.

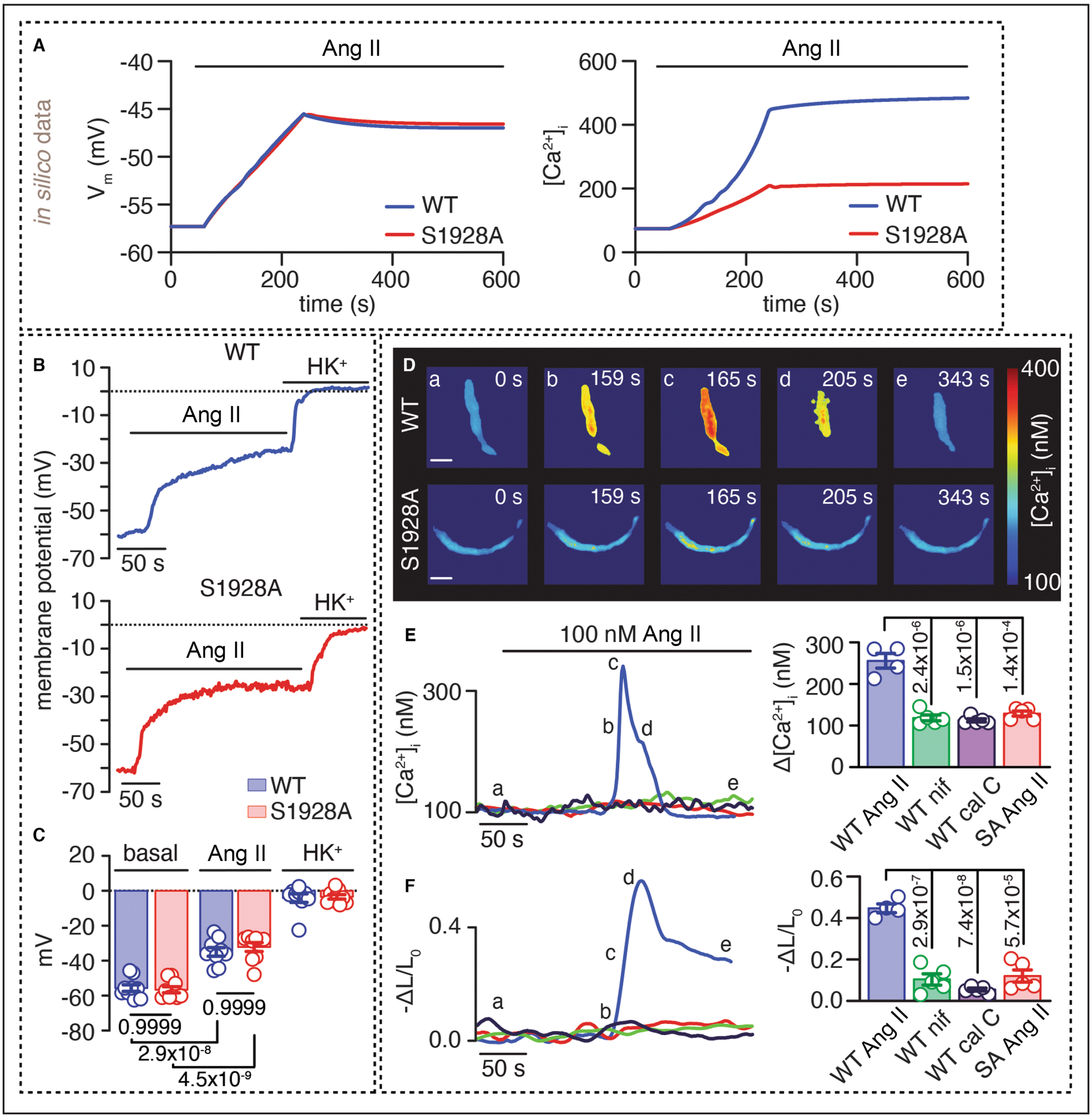

Figure 3. pS1928 mediates altered arterial myocyte excitation-contraction coupling upon Ang II.
A, Simulated Ang II-mediated effects on arterial myocyte V_M and $[Ca^{2+}]_i$. To simulate the gradual effects of Ang II over time, full modification of Ang II-dependent model parameters is reached after 180 seconds (s) from the initial administration. The mathematical model was parameterized using a 100% increase in Ca^{2+} currents, 60% reduction in K^+ currents and 75% increase in TRP currents upon Ang II exposure in WT cells, and 60% reduction in K^+ currents and 75% increase in TRP currents with no change in Ca^{2+} currents upon Ang II exposure in SA cells. The changes in Ca^{2+}, K^+, and TRP currents are consistent with prior data and results here.[3,7,43–46] **B**, Representative traces of perforated whole-cell recordings from WT and SA mesenteric arterial myocytes in current-clamp mode with a gap-free protocol and (**C**) summary data of V_M under control conditions and after exposure to 100 nmol/L Ang II and 60 mmol/L KCl (WT n=9 cells from 3 mice; SA n=9 cells from 3 mice). HK^+=60 mmol/L K^+. Significance was assessed with nested 2-way ANOVA with Bonferroni post hoc test (P=0.3882 in interaction and $P=7.9\times10^{-13}$ in treatment). **D**, Exemplary normalized pseudocolored confocal images at different time points and resulting fluorescence (**E**) and cell length (**F**) traces of WT and S1928A mesenteric arterial myocytes loaded with the fluorescent Ca^{2+} indicator fluo-4 AM. Summary data of (**E**) peak $[Ca^{2+}]_i$ and (**F**) cell length of WT and SA arterial myocytes after exposure to 100 nmol/L Ang II. In some experiments, WT cells were pre-treated with 100 nmol/L nif or 100 nmol/L calphostin C (cal C) before application of 100 nmol/L Ang II (WT Ang II: n=4 mice; WT Ang II+nif: n=5 mice; WT Ang II+cal C: n=5 mice; SA Ang II: n=5 mice). Significance was assessed with 1-way ANOVA with Bonferroni post hoc for comparisons between WT conditions ($P=1.4\times10^{-7}$ for 3E and $P=7.5\times10^{-8}$ for 3F). For comparisons between WT and SA conditions, unpaired *t* test was used. Data are mean±SEM. *P* values for relevant comparisons within each panel and supplemental material. Ang II indicates angiotensin II; $[Ca^{2+}]_i$, intracellular Ca^{2+} concentration; nif, nifedipine; pS1928, serine 1928 phosphorylation; SA, serine 1928 mutated to alanine; TRP, transient receptor potential; V_M, membrane potential; and WT, wild type.

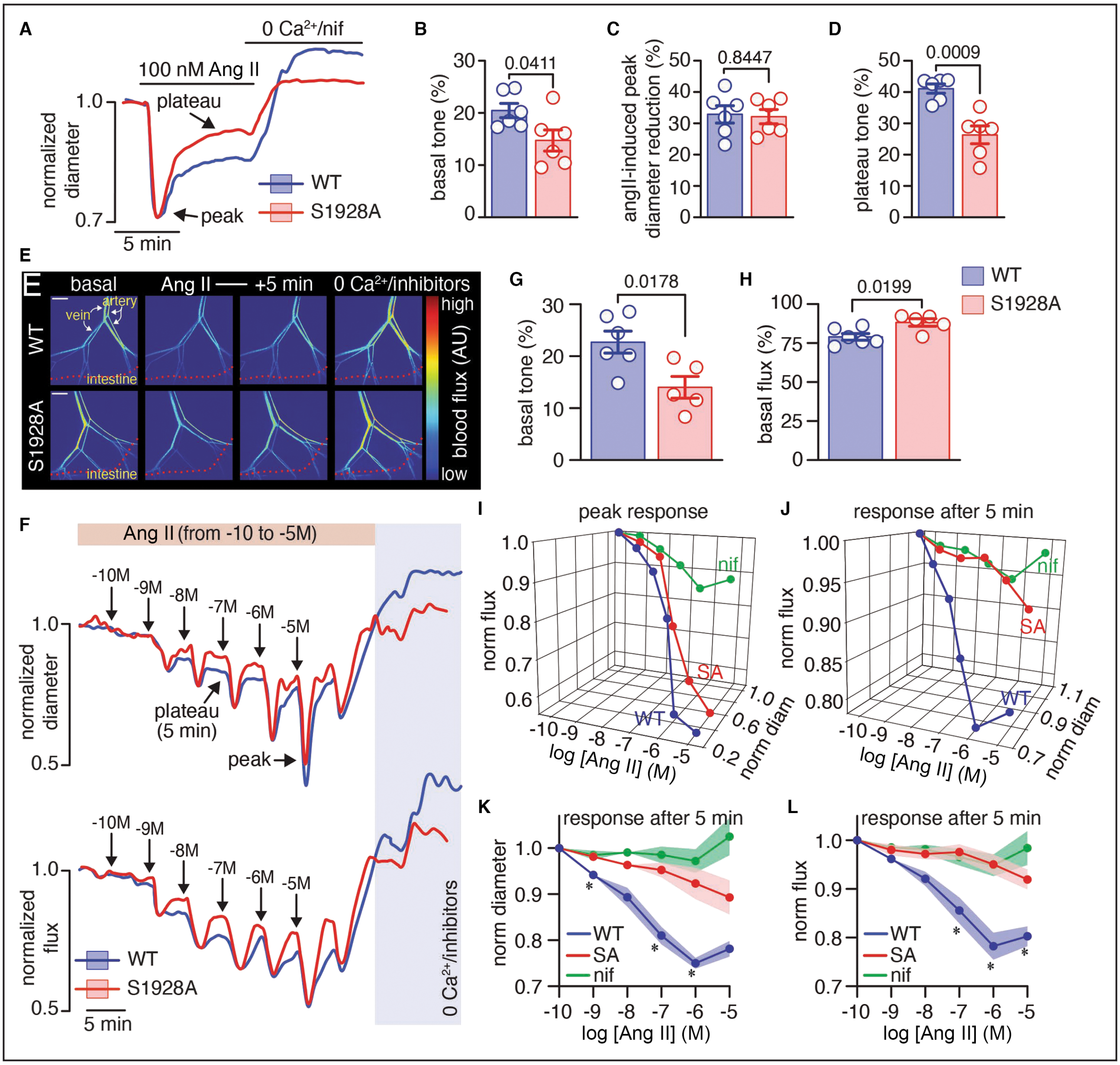

Figure 4. pS1928 sustains arterial constriction upon Ang II.

A, Representative normalized diameter traces of WT and SA male mesenteric arteries pressurized to 60 mm Hg and treated with 100 nmol/L Ang II and 0 Ca^{2+}+ 1 µmol/L nifedipine. The peak and plateau tones are highlighted by arrows. Scatter plots of (**B**) basal tone, (**C**) Ang II-induced peak diameter reduction, and (**D**) plateau tone (n=6 mice per group). Significance was assessed with unpaired *t* test for all plots. (**E**) Representative pseudocolored blood flow (ie, flux) images of WT and SA male mesenteric arteries through a laparotomy before and after exposure to Ang II and 0 Ca^{2+} plus a vasodilatory mix (described in the Methods section). (**F**) Exemplary normalized arterial diameter (*upper panel*) and normalized blood flux (*lower panel*) before and after exposure to increasing concentrations of Ang II (from log−10 mol/L to log−5 mol/L) and subsequent application of 0 Ca^{2+} plus a vasodilatory mix. **G** and **H**, Summary plots of basal tone and basal flux, respectively (n=6 mice per group). Significance was assessed with unpaired *t* test. **I** and **J**, Exemplary 3-dimensional graphs highlighting the peak and 5-minute normalized arterial diameter and blood flux responses, respectively, to the range of Ang II concentrations in mesenteric arteries from WT and SA male mice. In some experiments, mesenteric arteries from WT mice were pretreated with 1 µmol/L nifedipine before the application of the range of Ang II concentrations to examine the role of nifedipine-sensitive channels in Ang II-induced alterations in arterial diameter and blood flux in vivo. **K** and **L**, Amalgamated data of normalized diameter and blood flux, respectively, in mesenteric arteries from WT, WT+nifedipine, and SA male mice after 5 minutes in response to a range of Ang II concentrations (WT: n=8 mice; WT+nifedipine: n=8 mice; SA: n=7 mice). Significance was assessed with multiple unpaired *t* test (relevant comparisons between WT and SA data in Figure 4K: *P*=0.0197 at −9 M Ang II; *P*=0.0571 at −8 M Ang II; *P*=0.0004 at −7 M Ang II; *P*=0.0085 at −6 M Ang II; *P*=0.1250 at −5 M Ang II, and between WT and SA data in Figure 4L: *P*=0.9999 at −9 M Ang II; *P*=0.0817 at −8 M Ang II; *P*=0.0139 at −7 M Ang II; *P*=0.0018 at −6 M Ang II; *P*=0.0088 at −5 M Ang II). Data are mean±SEM. *P* values for relevant comparisons within each panel and supplemental material. Ang II indicates angiotensin II; nif, nifedipine; pS1928, serine 1928 phosphorylation; SA, serine 1928 mutated to alanine; and WT, wild type.

Laser speckle experiments in mesenteric arteries from WT female mice revealed lower basal tone and Ang II-induced changes in diameter and flux compared with male mice (Figure S7A through S7D), consistent with reported sex differences in these properties.[30] Moreover, while Ang II induced a concentration-dependent decrease in arterial diameter and concomitant reduction in blood flow (ie, flux) in mesenteric arteries from WT and S1928A female mice, preventing pS1928 did not lessen the Ang II response (Figure S7E through S7L). These results suggest sex-dependent differences in mechanisms by which Ang II modulates vascular function in vivo.

pS1928 Enhances Vascular $Ca_V1.2$ Activity and Cooperativity in Hypertension

Considering that chronic activation of Ang II signaling contributes to enhanced $Ca_V1.2$ channel activity and the development of hypertension,[3,5–11] we examined if pS1928 underlies the alterations in channel properties. Unitary data showed that channel nPo and availability were increased in WT hypertensive arterial myocytes compared with WT sham cells (Figure 5A and 5B and Figure S8). The frequency and strength (κ) of cooperative $Ca_V1.2$ events showed a robust trend toward higher values in WT hypertensive myocytes compared with WT sham cells (Figure 5C and 5D). The changes in $Ca_V1.2$ channel properties in WT hypertensive cells were not observed in S1928A hypertension compared with S1928A sham cells (Figure 5A through 6D; Figure S8). Moreover, channel nPo and availability, as well as coupling frequency and strength, were significantly higher in WT hypertension compared with S1928A hypertensive myocytes. These results suggest that pS1928 triggers increased vascular $Ca_V1.2$ channel function in male arterial myocytes during hypertension.

pS1928 Mediates Increased Vascular $\alpha1_C$ Clustering in Hypertension

We next examined if $\alpha1_C$ clustering was increased in freshly isolated male arterial myocytes during hypertension and if this process required pS1928. Superresolution imaging with pair-correlation analysis (Figure 5E and 5F) found an increase in $\alpha1_C$ cluster size (Figure 5G), no significant differences in cluster density (Figure 5H), and trends toward higher $N^{clusters}$ (Figure 5I) in WT hypertensive arterial myocytes compared with WT sham and S1928A HTN cells. These changes were not observed in S1928A hypertensive cells compared with S1928A sham, which had similar $\alpha1_C$ cluster properties as WT sham (Figure 5E through 5I). The modified PLA assay confirmed the increase in $\alpha1_C$ clustering in WT hypertension compared with WT sham, and S1928A sham and hypertensive cells (Figure 5J; Figure S9). No PLA signal was detected when one of the primary antibody-probe complexes was omitted from the preparation (Figure 5J; Figure S9). Intriguingly, no change in total $\alpha1_C$ protein abundance was detected by Western blot in WT and S1928A hypertensive lysates compared with sham conditions (Figure S10). These results were unexpected as prior studies have shown increased total $\alpha1_C$ protein abundance in arterial lysates during hypertension.[5] Results may point to offsetting changes, possibly associated with the hypertension model.[5] Regardless, these results indicate that $\alpha1_C$ clustering properties in male arterial myocytes are elevated during hypertension, and this spatial remodeling is mediated by pS1928.

To examine if similar increases in $\alpha1_C$ clustering were observed in different models of hypertension, superresolution experiments were performed using male arterial myocytes from the BPH compared to BPN mice. Hypertension in BPH mice is thought to be mediated

Figure 5. Increased $Ca_V1.2$ activity and $\alpha1_C$ clustering during hypertension.
A, Scatter plots of (**A**) channel activity (nPo), (**B**) channel availability, (**C**) coupling frequency and (**D**) coupling strength (κ) in sham and hypertension WT and SA arterial myocytes (WT sham: n=15 cells from 5 mice; WT hypertension: n=16 cells from 7 mice; SA sham: n=11 cells from 4 mice; SA hypertension: n15 cells from 5 mice). Significance was assessed with nested 2-way ANOVA with Bonferroni post hoc test (P=0.0054 for **A**; P=0.0068 for **B**; P=0.1721 for interaction and P=0.0099 for treatment for **C**; P=0.4589 for interaction and P=0.0001 for treatment for **D**). **E**, Representative super- TIRF images of sham and hypertension WT and SA arterial myocytes labeled for $\alpha1_C$ with 2 magnified areas (scale bars=5 µm→200 nm). **F**, Plot of the calculated pair-correlation function (g(r)) of $\alpha1_C$ clusters in sham and hypertension WT and SA arterial myocytes. Scatter plots of (**G**) $\alpha1_C$ cluster radius (nm), (**H**) $\alpha1_C$ cluster density (number of cluster/µm^2) and (**I**) estimated $\alpha1_C$ proteins per cluster ($N^{cluster}$) in sham and hypertension WT and SA arterial myocytes (WT sham: n=16 cells from 5 mice; WT hypertension: n=37 cells from 6 mice; SA sham: n=25 cells from 6 mice; SA hypertension: n=26 cells from 6 mice). Significance was assessed with nested 2-way ANOVA with Bonferroni post hoc test (P=0.0216 for **G**; P=0.9509 for **H**; P=0.6589 for interaction and 0.0056 for genotype for **I**). **J**, Scatter plot of PLA $\alpha1_C$-$\alpha1_C$ puncta per cell area (µm^2) in sham and hypertension WT and SA arterial myocytes (WT sham: n=29 cells from 6 mice; WT hypertension: n=50 cells from 7 mice; SA sham: n=28 cells from 5 mice; SA hypertension: n=27 cells from 5 mice). WT sham arterial myocytes treated with only 1 of the PLA probes were used as negative control (neg ct; n=4 cells from 2 mice). Significance was assessed with nested 2way ANOVA with Bonferroni post hoc test (P=0.0252). **K**, Representative superresolution TIRF images of BPN and BPH arterial myocytes labeled for $\alpha1_C$ with 2 magnified areas (scale bars=5 µm→200 nm). Scatter plots of (**L**) $\alpha1_C$ cluster radius (nm), (**M**) $\alpha1_C$ cluster density (number of cluster/µm^2), and (**I**) estimated $\alpha1_C$ proteins per cluster ($N^{cluster}$) in BPN and BPH arterial myocytes (BPN: n=47 cells from 5 mice; BPH: n=47 cells from 6 mice). Significance was assessed with nested *t* test. Data are mean±SEM. *P* values for relevant comparisons within each panel and supplemental material. BPH indicates blood pressure highp; BPN, blood pressure normal; ct, control conditions; HTN, hypertension; nPO, number of channels X open probability; PLA, proximity ligation assay; SA, serine 1928 mutated to alanine; TIRF, total internal reflection fluorescence; and WT, wild type.

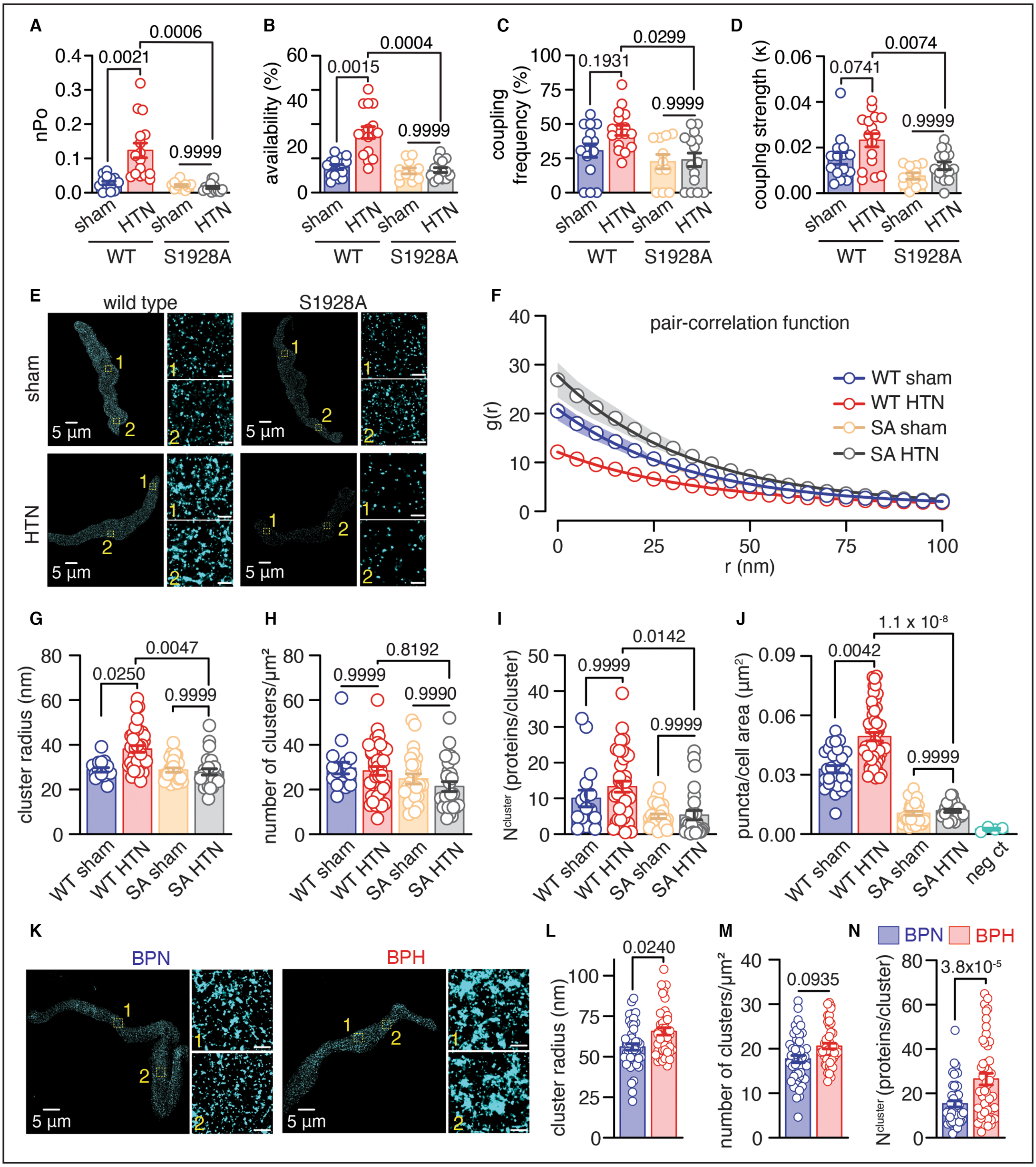

by sympathetic overactivity,[47] which acting through the α-adrenergic receptors/PKC axis, may modulate $\alpha1_C$ clustering. Data show that $\alpha1_C$ clustering is increased in BPH arterial myocytes compared with BPN cells (Figure 5K through 5M). The $\alpha1_C$ superclustering in BPH arterial myocytes correlated with increased $Ca_V1.2$ nPo and cooperativity previously reported in these cells.[48] Moreover, in pressurized arteries, noradrenaline caused an initial peak constriction of similar magnitude in WT and S1928A vessels (Figure S11). Yet, in the continuous presence of noradrenaline, WT arteries reached a steady-state level (eg, plateau level) with higher vascular tone compared with S1928A arteries (Figure S11). These results are consistent with the Ang II observations here and prior studies indicating that noradrenaline increases L-type Ca^{2+} channel activity leading to enhanced vascular tone[49] and suggest that noradrenaline-induced elevation in steady-state tone in

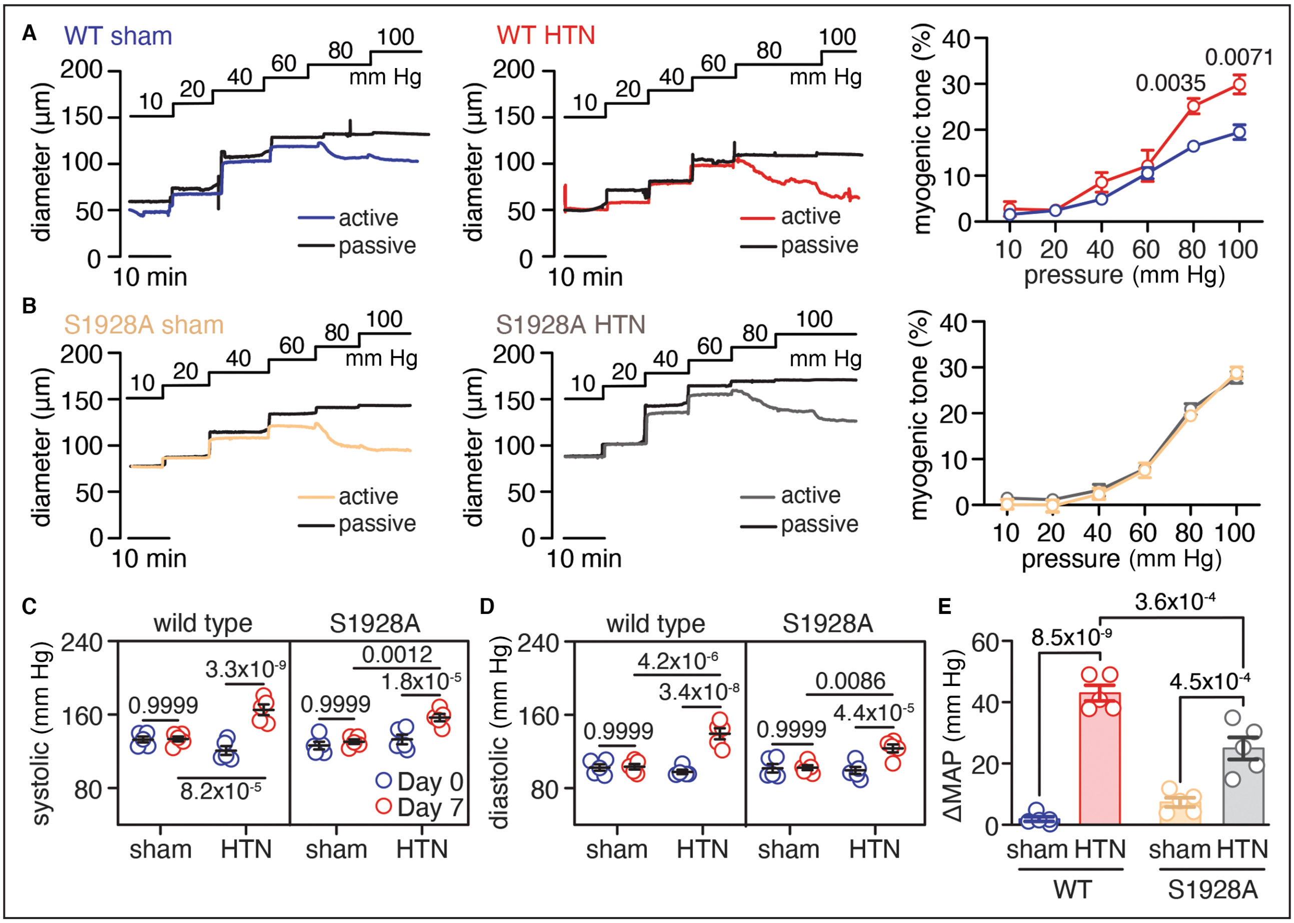

Figure 6. pS1928 regulates $Ca_V1.2$ function, vascular reactivity, and blood pressure during hypertension.
Representative diameter recordings over a pressure range (from 10 to 100 mm Hg) and plot summary data of percentage myogenic tone obtained using mesenteric arteries from WT (**A**) and SA (**B**) sham and hypertension mice (WT sham: n=12 arteries from 5 mice; WT hypertension: n=9 arteries from 5 mice; SA sham: n=8 arteries from 5 mice; S1928A hypertension: n=7 arteries from 5 mice). Significance was assessed with nested *t*-test. Plots of systemic (**C**) and diastolic (**D**) blood pressure at day 0 (blue circles) and day 7 (red circles) from sham and hypertensive WT and SA mice using radio telemetry (n=5 mice per group). Significance was assessed with 3-way ANOVA with Bonferroni post hoc test (*P*=0.0017 for **C**; *P*=0.0299 for **D**). **E**, Scatter plot of ΔMAP from day 0 to day 7 in sham and hypertensive WT and SA mice (n=5 mice per group). Significance was assessed with 2-way ANOVA with Bonferroni post hoc test ($P=1.4\times10^{-4}$). Data are mean±SEM. *P* values for relevant comparisons within each panel and supplemental material. ΔMAP, change in mean arterial pressure; HTN, hypertension; pS1928, serine 1928 phosphorylation; SA, serine 1928 mutated to alanine; WT, wild type.

mesenteric arteries requires $\alpha1_C$ S1928 phosphorylation. Results further indicate that enhanced $\alpha1_C$ clustering may be a general feature in hypertensive arterial myocytes to increase $Ca_V1.2$ activity and cooperativity, and vascular tone.

pS1928 Underlies Increased Myogenic Tone and Blood Pressure in Hypertension

To establish the physiological relevance of pS1928 during hypertension, we measured myogenic tone in pressurized male mesenteric arteries. We found that WT hypertensive arteries developed higher myogenic tone at physiologically relevant intravascular pressures (ie, >60 mm Hg) than WT sham arteries (Figure 6A). The hypertension-induced elevations in myogenic tone were not observed when comparing tone levels in S1928A sham and hypertensive arteries (Figure 6B). These results suggest that elevations in myogenic tone in male mesenteric arteries during hypertension require pS1928.

Lastly, we examined the role of pS1928 in BP regulation in freely moving WT and S1928A male mice implanted with radiotelemetry devices and osmotic minipumps eluting either saline (ie, sham) or Ang II (ie, hypertension). BP measurements were analyzed at day 0 and day 7 after minipump implantation. Telemetry data showed that resting (Day 0) systolic pressure (Figure 6C), diastolic pressure (Figure 6D), and mean arterial pressure (MAP; Figure S12A) were similar in WT and S1928A mice. However, a significant increase in systolic pressure (Figure 6C), diastolic pressure (Figure 6D), and MAP (Figure S12A) was observed in both WT and S1928A mice after 7 days with a minipump eluting Ang II compared with saline. The increase in MAP in S1928A hypertensive mice was not surprising as BP is regulated by many factors in addition to peripheral vascular resistance, such as alterations in sympathetic activity, baroreflex dysfunction, or renal abnormalities. Importantly, the change in MAP (ΔMAP) during hypertension was significantly larger in WT mice compared with S1928A mice (Figure 6E). These results are remarkable in that preventing phosphorylation of a single amino acid in $\alpha 1_C$ significantly ameliorates Ang II-induced hypertension. Note that, in our hands, pulse pressure (an indicator of arterial stiffness and cardiac contraction; Figures S12B), heart rate (Figure S12C), and cardiac hemodynamics (Figure S12D through S12G) were similar in WT and S1928A sham and hypertensive mice. Overall, these results suggest that pS1928 contributes to increasing BP without a major impact on cardiac function in an Ang II-induced hypertensive male mouse model.

DISCUSSION

We report 5 key findings (Figure 7). First, the $\alpha 1_C$ subunit of the $Ca_V1.2$ channel in WT male arterial myocytes exposed to Ang II or from the Ang II-induced hypertension, as well as genetically induced hypertensive (eg, BPH) mice reorganizes into larger clusters (ie, $\alpha 1_C$ superclusters), and this requires PKC. Second, the $\alpha 1_C$ superclustering leads to an increase in $Ca_V1.2$ channel current density and the frequency and strength of $Ca_V1.2$ cooperative events. Third, $\alpha 1_C$ S1928 phosphorylation mediates the spatial reorganization of vascular $\alpha 1_C$ into superclusters, as well as the increase in $Ca_V1.2$ current density and cooperativity during Ang II exposure and hypertension as concluded using cells/tissue from S1928A mice. Fourth, $\alpha 1_C$ S1928 phosphorylation underlies a PKC-dependent increase in male arterial myocyte $[Ca^{2+}]_i$ and contractility, leading to enhanced myogenic tone in arteries exposed to Ang II and from WT male hypertensive mice (also concluded using cells/tissue from S1928A mice). Fifth, $\alpha 1_C$ S1928 phosphorylation contributes to hypertension as determined by a reduced change in mean arterial pressure when comparing WT and S1928A mice. These results uncovered a previously unappreciated role for pS1928 in mediating a PKC-dependent spatiotemporal regulation of vascular $Ca_V1.2$ channels to alter vascular reactivity and BP during activation of Ang II signaling and hypertension. We propose that pS1928 is a rheostat of vascular

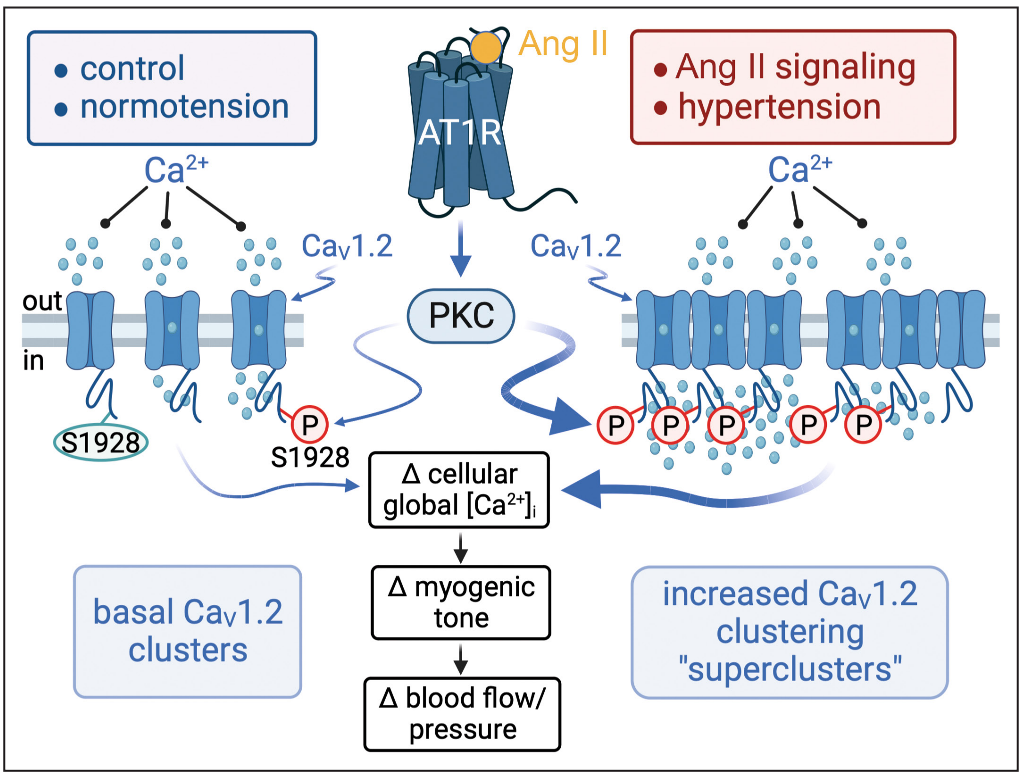

Figure 7. Model by which Ang II/PKC signaling promotes α_{1C} pS1928 to modulate the $\alpha 1_C/Ca_V1.2$ channel spatial and temporal properties leading to changes in global $[Ca^{2+}]_i$, myogenic tone, blood flow, and blood pressure during hypertension.

Image created with Biorender.com. Ang II indicates angiotensin II; $[Ca^{2+}]_i$, intracellular Ca^{2+} concentration; PKC, protein kinase C; pS1928, serine 1928 phosphorylation; and S1928, serine 1928.

$Ca_V1.2$ function and vascular reactivity and a risk factor for hypertension.

Prior work in heterologous expression systems suggested the possibility that $Ca_V1.2$ channels could be in complex with PKC to promote phosphorylation of $\alpha1_C$ at S1928 to alter channel function.[24,25] Our findings support this premise, as they revealed a key role for pS1928 in mediating changes in $\alpha1_C/Ca_V1.2$ spatiotemporal properties in response to Ang II/PKC signaling and hypertension. These results are significant because they uncover previously unappreciated mechanisms by which Ang II/PKC signaling may alter vascular $\alpha1_C/Ca_V1.2$ function and vascular reactivity in health and hypertension. Given that diabetic hyperglycemia has been found to elevate pS1928 levels,[18,20,28] it raises the intriguing possibility that this α_{1C} amino acid may serve as a "pathological hub" mediating vascular dysfunction in various diseases.

The current general model of $Ca_V1.2$ cooperativity suggests the stochastic, Ca^{2+}-dependent self-assembly of $\alpha1_C$ in clusters of various sizes at the plasma membrane.[4,50] Our findings have important implications as they provide evidence that pS1928 is necessary for the PKC (but not PKA)-dependent spatial reorganization of $\alpha1_C$ subunits into superclusters during acute Ang II and hypertension (Figures 2 and 5; Figure S4). This $\alpha1_C$ spatial remodeling upon Ang II exposure and hypertension was correlated with increased $Ca_V1.2$ function (Figures 1 and 5). Supporting a central role for PKC and its anchoring near $Ca_V1.2$ in this process, few to no changes in $Ca_V1.2$ properties were observed in PKCα knockout (PKCα$^{-/-}$) or AKAP5 knockout (AKAP5$^{-/-}$) arterial myocytes acutely exposed to Ang II or from Ang II-infused PKCα$^{-/-}$ and AKAP5$^{-/-}$ mice.[3,7,20] Caveolin may also play a structural or signaling role in regulating $Ca_V1.2$ function, which remains to be determined. The results highlight the key involvement of $\alpha1_C$ pS1928 in the spatiotemporal regulation (ie, clustering and cooperativity) of vascular $Ca_V1.2$ channels upon activation of Ang II/PKC signaling and hypertension. Moreover, considering that vascular $\alpha1_C$ S1928 is a substrate for both PKA and PKC phosphorylation, we propose that this site is a master regulator of vascular $Ca_V1.2$ channel function. Future studies should assess how PKA and PKC may differentially regulate $\alpha1_C/Ca_V1.2$, which may involve spatial segregation of G_S versus G_q protein-coupled receptors with specific subpopulations of the channel.

An emerging and important concept is that $Ca_V1.2$ channels can be distinctively regulated in different cell types. Intriguingly, a recent study found that acute Ang II exposure of freshly isolated cardiomyocytes resulted in reduced surface expression and cluster size of cardiac $\alpha1_C$.[51] This was correlated with a decrease in $Ca_V1.2$ current density and Ca^{2+} transients in cardiomyocytes. In stark contrast, our study shows that acute and chronic Ang II exposure increased vascular $\alpha1_C$ clustering and $Ca_V1.2$ function, which was associated with increased arterial myocyte $[Ca^{2+}]_i$ and contractility. In addition, whereas Ang II regulation of $\alpha1_C/Ca_V1.2$ was linked to the depletion of the membrane phospholipid phosphatidylinositol 4,5 bisphosphate in cardiomyocytes,[51] pS1928 was required in arterial myocytes. These contrasting Ang II effects on cardiac versus vascular $\alpha1_C/Ca_V1.2$ (and underlying functional impact) provide additional evidence supporting the tissue-specific regulation of this important ion channel. Although the mechanisms mediating $\alpha1_C/Ca_V1.2$ tissue-specific regulation are unclear, they could involve the expression of different $\alpha1_C$ splice variants or distinct lipid microenvironments in cardiac versus vascular tissue. Regardless, these fundamental differences may be exploited to treat hypertension without affecting cardiac function.

A significant outcome of pS1928-mediated $\alpha1_C$ superclustering and increased $Ca_V1.2$ function in Ang II/PKC signaling activation and hypertension is the underlying amplification of Ca^{2+} influx, which may alter cellular and tissue responses.[2,4] Accordingly, this study linked the pS1928-induced $\alpha1_C$ superclustering and $Ca_V1.2$ channel function to elevations in arterial myocyte $[Ca^{2+}]_i$ and contraction in response to acute Ang II (Figure 3) and hypertension (Figure 5). Inhibiting PKC in WT cells and blocking pS1928 (as in S1928A cells) prevented the Ang II-induced elevation of arterial myocyte $[Ca^{2+}]_i$ and contraction. The results are significant because they suggest a direct link between PKC and pS1928 in modulating arterial myocyte $[Ca^{2+}]_i$ and contraction during Ang II signaling. At the tissue level, however, acute Ang II induced an initial constriction of similar magnitude in both WT and S1928A arteries in ex vivo and in vivo preparations (Figure 4). By contrast, the cellular data in S1928A arterial myocytes showed no significant changes in cell length (ie, contraction) to Ang II exposure. This unexpected result may reflect the complex interplay between different cells and signaling pathways that could be engaged by Ang II exposure in intact tissue versus isolated arterial myocytes. Nonetheless, the vascular and myogenic response was elevated in WT compared with S1928A tissue (both ex vivo and in vivo) after continued exposure to Ang II and during hypertension, which correlated with concomitant yet contrasting changes in blood flow and BP (Figures 4 and 6). The results are comparable with prior work from our group showing that genetic ablation of PKCα or AKAP5 ameliorates Ang II-induced elevation in BP,[3,7] thus providing a link between activation of AKAP5-anchored PKC near vascular $Ca_V1.2$ and pS1928 in control of BP. The differences in ΔMAP between WT and S1928A hypertensive mice were not mediated by alterations in heart function, as heart rate and cardiac hemodynamics were similar between these cohorts of mice (Figure S12D through S12G). Overall, data here suggest a key role and strong connection between the spatiotemporal regulation of vascular $\alpha1_C/Ca_V1.2$ and the underlying cellular/tissue responses to control blood flow and BP in hypertension, which is mediated by pS1928. Given that preventing pS1928 ameliorates hypertension, this $\alpha1_C$ amino acid may be a new therapeutic target that could help correct $Ca_V1.2$ dysfunction and ameliorate vascular complications.

Increased $Ca_V1.2$ function leading to Ca^{2+} influx amplification in arterial myocytes may also regulate excitation-transcription coupling.[4] Thus, increased $Ca_V1.2$ channel function upon Ang II signaling activation during hypertension may engage the prohypertensive transcriptional cascade involving calcineurin and NFATc3 (nuclear factor of activated T cells 3).[3,43,44] Consistent with this, calcineurin and NFATc3 activation are enhanced in arterial myocytes from Ang II-induced hypertensive mice.[43] NFATc3 activation in hypertensive arterial myocytes led to the selective downregulation of several K^+ channel subunits, including the BKβ1 and $K_V2.1$ subunits.[43,44] The NFATc3 activation and downregulation of K^+ channel subunits in hypertensive arterial myocytes was blocked by the $Ca_V1.2$ channel blocker nifedipine, providing a link between $Ca_V1.2$ function, NFATc3 signaling, and transcriptional regulation.[43] It is intriguing to speculate that blocking pS1928 will prevent not only enhanced $Ca_V1.2$ channel function but also activation of the calcineurin/NFATc3 pathway and underlying transcriptional changes in K^+ channel functional expression. Future studies should examine these possibilities.

Although we confirmed an increase in $\alpha1_C$ superclustering in 2 models of hypertension (Ang II-induced hypertension and BPH), all other experimental series were examined using the Ang II-induced hypertension model. Additional experiments in samples from other hypertension models and patients with hypertension will be useful to ascertain the general impact of pS1928 in modulating $Ca_V1.2$ activity, vascular function, and BP. While this study provides strong functional data highlighting the importance of pS1928, we were not able to provide direct evidence of changes in the phosphorylation state of the site due to the unavailability of well-validated antibodies, which should be addressed in future studies. The role of pS1928 in $\alpha1_C$ trafficking, which may contribute to $\alpha1_C$ superclustering,[52,53] will have to be investigated. Our data also highlight distinct basal and sex-dependent responses to Ang II. These results suggest that distinctive mechanisms may be engaged in the regulation of $\alpha1_C/Ca_V1.2$ spatiotemporal properties and vascular function in males versus females, which may contribute to the observed sex differences in Ang II-induced hypertension.[30] Accordingly, recent studies suggest that $\alpha1_C$ superclusters in female arterial myocytes are sustained by a concomitant self-assembly superclustering of $K_V2.1$ channels due to increased phosphorylation of S590 in $K_V2.1$ channels.[54,55] These sex-dependent changes in $K_V2.1$-dependent $\alpha1_C$ clustering may be driven by sex hormones and affected by age, which can then influence vascular function and BP/flow control.[56,57] These observations and results here may inspire future studies to comprehensively compare the sex- and age-dependent role of $\alpha1_C$ pS1928 and $K_V2.1$ pS590 in modulating $\alpha1_C/Ca_V1.2$, vascular function, and BP during basal conditions and hypertension.

CONCLUSIONS

In summary, the findings here identify $\alpha1_C$ S1928 as a target for Ang II/PKC signaling in native vascular tissue. Data also indicate that pS1928 mediates a spatiotemporal remodeling of vascular $\alpha1_C/Ca_V1.2$ to control arterial myocyte $[Ca^{2+}]_i$ and contraction, leading to alterations in vascular reactivity, blood flow, and BP during hypertension. Results are highly significant, as they reveal a previously unappreciated mechanism contributing to pathological changes in a crucial ion channel central for regulating cardiovascular function, thus providing a potential new target for developing novel therapeutics aimed at controlling hypertension.

ARTICLE INFORMATION

Received May 24, 2024; accepted August 5, 2024.

Affiliations

Department of Pharmacology (V.A.F., M.M.B., J.H., J.L.T., L.R., T.L., A.U.S., Y.M., N.S., W.R.L., G.R.R., V.R., K.N.M., P.B., Y.C., C-Y.C., S.M., E.G., J.W.H., M.C.H., M.N., M.F.N.), Department of Cell Biology & Human Anatomy (S.S.) and Department of Physiology & Membrane Biology, University of California Davis, Davis, CA (E.J.D., L.F.S.).

Acknowledgments

The authors thank Hannah Voorhees and Zolia Estrada-Tobar for technical support. This work is dedicated to the memory of Manuel F. Navedo Sr (Mi Querido Viejo!).

Sources of Funding

This work was supported by National Institutes of Health grants R01HL149127, R01HL121059, R01HL171014 and R01HL161872 (to Manuel F. Navedo), and R00HL138160 (to Stefano Morotti), and American Heart Association Postdoctoral Fellowship 830629 (to Miguel Martín-Aragón Baudel) and 1022782 (to Jade L. Taylor) as well as an American Heart Association Career Development Award 852984 (to Madeline Nieves-Cintrón). Madeline Nieves-Cintrón is a University of California Davis CAMPOS Fellow.

Disclosures

None.

Supplemental Material

Data S1
Table S1
Figures S1–S12

REFERENCES

1. Hofmann F, Flockerzi V, Kahl S, Wegener JW. L-type CaV1.2 calcium channels: from in vitro findings to in vivo function. *Physiol Rev*. 2014;94:303–326. doi: 10.1152/physrev.00016.2013

2. Ghosh D, Syed AU, Prada MP, Nystoriak MA, Santana LF, Nieves-Cintron M, Navedo MF. Calcium channels in vascular smooth muscle. *Adv Pharmacol*. 2017;78:49–87. doi: 10.1016/bs.apha.2016.08.002
3. Nieves-Cintron M, Amberg GC, Navedo MF, Molkentin JD, Santana LF. The control of Ca^{2+} influx and NFATc3 signaling in arterial smooth muscle during hypertension. *Proc Natl Acad Sci USA*. 2008;105:15623–15628. doi: 10.1073/pnas.0808759105
4. Dixon RE, Navedo MF, Binder MD, Santana LF. Mechanisms and physiological implications of cooperative gating of clustered ion channels. *Physiol Rev*. 2022;102:1159–1210. doi: 10.1152/physrev.00022.2021
5. Sonkusare S, Palade PT, Marsh JD, Telemaque S, Pesic A, Rusch NJ. Vascular calcium channels and high blood pressure: pathophysiology and therapeutic implications. *Vasc Pharmacol*. 2006;44:131–142. doi: 10.1016/j.vph.2005.10.005
6. Navedo MF, Cheng EP, Yuan C, Votaw S, Molkentin JD, Scott JD, Santana LF. Increased coupled gating of L-type Ca^{2+} channels during hypertension and Timothy syndrome. *Circ Res*. 2010;106:748–756. doi: 10.1161/CIRCRESAHA.109.213363
7. Navedo MF, Nieves-Cintron M, Amberg GC, Yuan C, Votaw VS, Lederer WJ, McKnight GS, Santana LF. AKAP150 is required for stuttering persistent Ca^{2+} sparklets and angiotensin II-induced hypertension. *Circ Res*. 2008;102:e1–e11. doi: 10.1161/CIRCRESAHA.107.167809
8. Pratt PF, Bonnet S, Ludwig LM, Bonnet P, Rusch NJ. Upregulation of L-type Ca^{2+} channels in mesenteric and skeletal arteries of SHR. *Hypertension*. 2002;40:214–219. doi: 10.1161/01.HYP.0000025877.23309.36
9. Wynne BM, Chiao CW, Webb RC. Vascular smooth muscle cell signaling mechanisms for contraction to angiotensin II and Endothelin-1. *J Am Soc Hypertens*. 2009;3:84–95. doi: 10.1016/j.jash.2008.09.002
10. Mehta PK, Griendling KK. Angiotensin II cell signaling: physiological and pathological effects in the cardiovascular system. *Am J Physiol Cell Physiol*. 2007;292:C82–C97. doi: 10.1152/ajpcell.00287.2006
11. Catt KJ, Cran E, Zimmet PZ, Best JB, Cain MD, Coghlan JP. Angiotensin II blood-levels in human hypertension. *Lancet*. 1971;1:459–464. doi: 10.1016/S0140-6736(71)91085-3
12. Touyz RM, Schiffrin EL. Signal transduction mechanisms mediating the physiological and pathophysiological actions of angiotensin II in vascular smooth muscle cells. *Pharmacol Rev*. 2000;52:639–672.
13. Salamanca DA, Khalil RA. Protein kinase C isoforms as specific targets for modulation of vascular smooth muscle function in hypertension. *Biochem Pharmacol*. 2005;70:1537–1547. doi: 10.1016/j.bcp.2005.07.017
14. Fransen P, Van Hove CE, Leloup AJ, Schrijvers DM, De Meyer GR, De Keulenaer GW. Effect of angiotensin II-induced arterial hypertension on the voltage-dependent contractions of mouse arteries. *Pflugers Arch*. 2016;468:257–267. doi: 10.1007/s00424-015-1737-x
15. Liu G, Papa A, Katchman AN, Zakharov SI, Roybal D, Hennessey JA, Kushner J, Yang L, Chen BX, Kushnir A, et al. Mechanism of adrenergic CaV1.2 stimulation revealed by proximity proteomics. *Nature*. 2020;577:695–700. doi: 10.1038/s41586-020-1947-z
16. Manning JR, Yin G, Kaminski CN, Magyar J, Feng HZ, Penn J, Sievert G, Thompson K, Jin JP, Andres DA, et al. Rad GTPase deletion increases L-type calcium channel current leading to increased cardiac contraction. *J Am Heart Assoc*. 2013;2:e000459. doi: 10.1161/JAHA.113.000459
17. Qian H, Patriarchi T, Price JL, Matt L, Lee B, Nieves-Cintron M, Buonarati OR, Chowdhury D, Nanou E, Nystoriak MA, et al. Phosphorylation of Ser1928 mediates the enhanced activity of the L-type Ca^{2+} channel Cav1.2 by the β2-adrenergic receptor in neurons. *Sci Signal*. 2017;10:eaaf9659. doi: 10.1126/scisignal.aaf9659
18. Prada MP, Syed AU, Buonarati OR, Reddy GR, Nystoriak MA, Ghosh D, Simo S, Sato D, Sasse KC, Ward SM, et al. A Gs-coupled purinergic receptor boosts Ca(2+) influx and vascular contractility during diabetic hyperglycemia. *elife*. 2019;8. doi: 10.7554/eLife.42214
19. Patriarchi T, Qian H, Di Biase V, Malik ZA, Chowdhury D, Price JL, Hammes EA, Buonarati OR, Westenbroek RE, Catterall WA, et al. Phosphorylation of Cav1.2 on S1928 uncouples the L-type Ca^{2+} channel from the beta2 adrenergic receptor. *EMBO J*. 2016;35:1330–1345. doi: 10.15252/embj.201593409
20. Nystoriak MA, Nieves-Cintron M, Patriarchi T, Buonarati OR, Prada MP, Morotti S, Grandi E, Fernandes JD, Forbush K, Hofmann F, et al. Ser1928 phosphorylation by PKA stimulates the L-type Ca^{2+} channel CaV1.2 and vasoconstriction during acute hyperglycemia and diabetes. *Sci Signal*. 2017;10. doi: 10.1126/scisignal.aaf9647
21. Murphy JG, Sanderson JL, Gorski JA, Scott JD, Catterall WA, Sather WA, Dell'Acqua ML. AKAP-anchored PKA maintains neuronal L-type calcium channel activity and NFAT transcriptional signaling. *Cell Rep*. 2014;7:1577–1588. doi: 10.1016/j.celrep.2014.04.027
22. Keef KD, Hume JR, Zhong J. Regulation of cardiac and smooth muscle Ca2+channels (CaV1.2a,b) by protein kinases. *Am J Physiol Cell Physiol*. 2001;281:C1743–C1756. doi: 10.1152/ajpcell.2001.281.6.C1743
23. Weiss S, Dascal N. Molecular aspects of modulation of L-type calcium channels by protein kinase C. *Curr Mol Pharmacol*. 2015;8:43–53. doi: 10.2174/1874467208666150507094733
24. Yang L, Liu G, Zakharov SI, Morrow JP, Rybin VO, Steinberg SF, Marx SO. Ser1928 is a common site for Cav1.2 phosphorylation by protein kinase C isoforms. *J Biol Chem*. 2005;280:207–214. doi: 10.1074/jbc.M410509200
25. Raifman TK, Kumar P, Haase H, Klussmann E, Dascal N, Weiss S. Protein kinase C enhances plasma membrane expression of cardiac L-type calcium channel, CaV1.2. *Channels (Austin)*. 2017;11:604–615. doi: 10.1080/19336950.2017.1369636
26. van der Heyden MA, Wijnhoven TJ, Opthof T. Molecular aspects of adrenergic modulation of cardiac L-type Ca^{2+} channels. *Cardiovasc Res*. 2005;65:28–39. doi: 10.1016/j.cardiores.2004.09.028
27. Syed AU, Reddy GR, Ghosh D, Prada MP, Nystoriak MA, Morotti S, Grandi E, Sirish P, Chiamvimonvat N, Hell JW, et al. Adenylyl cyclase 5-generated cAMP controls cerebral vascular reactivity during diabetic hyperglycemia. *J Clin Invest*. 2019;129:3140–3152. doi: 10.1172/JCI124705
28. Martin-Aragon Baudel M, Flores-Tamez VA, Hong J, Reddy GR, Maillard P, Burns AE, Man KNM, Sasse KC, Ward SM, Catterall WA, et al. Spatiotemporal control of vascular Ca(V)1.2 by alpha1(C) S1928 phosphorylation. *Circ Res*. 2022;131:1018–1033. doi: 10.1161/CIRCRESAHA.122.321479
29. Lemke T, Welling A, Christel CJ, Blaich A, Bernhard D, Lenhardt P, Hofmann F, Moosmang S. Unchanged beta-adrenergic stimulation of cardiac L-type calcium channels in Ca v 1.2 phosphorylation site S1928A mutant mice. *J Biol Chem*. 2008;283:34738–34744. doi: 10.1074/jbc.M804981200
30. Xue B, Johnson AK, Hay M. Sex differences in angiotensin II- induced hypertension. *Braz J Med Biol Res*. 2007;40:727–734. doi: 10.1590/s0100-879x2007000500018
31. Le T, Martin-Aragon Baudel M, Syed A, Singhrao N, Pan S, Flores-Tamez VA, Burns AE, Man KNM, Karey E, Hong J, et al. Secondhand smoke exposure impairs ion channel function and contractility of mesenteric arteries. *Function (Oxf)*. 2021;2:zqab041. doi: 10.1093/function/zqab041
32. Kapela A, Bezerianos A, Tsoukias NM. A mathematical model of Ca^{2+} dynamics in rat mesenteric smooth muscle cell: agonist and NO stimulation. *J Theor Biol*. 2008;253:238–260. doi: 10.1016/j.jtbi.2008.03.004
33. Morotti S, Nieves-Cintron M, Nystoriak MA, Navedo MF, Grandi E. Predominant contribution of L-type Cav1.2 channel stimulation to impaired intracellular calcium and cerebral artery vasoconstriction in diabetic hyperglycemia. *Channels (Austin)*. 2017;11:340–346. doi: 10.1080/19336950.2017.1293220
34. Nystoriak MA, Nieves-Cintron M, Nygren PJ, Hinke SA, Nichols CB, Chen CY, Puglisi JL, Izu LT, Bers DM, Dell'acqua ML, et al. AKAP150 contributes to enhanced vascular tone by facilitating large-conductance Ca^{2+}–activated K^+ channel remodeling in hyperglycemia and diabetes mellitus. *Circ Res*. 2014;114:607–615. doi: 10.1161/CIRCRESAHA.114.302168
35. Eisner DA. Pseudoreplication in physiology: more means less. *J Gen Physiol*. 2021;153:153. doi: 10.1085/jgp.202012826
36. Seki T, Yokoshiki H, Sunagawa M, Nakamura M, Sperelakis N. Angiotensin II stimulation of Ca^{2+}-channel current in vascular smooth muscle cells is inhibited by lavendustin-a and LY-294002. *Pflugers Arch*. 1999;437:317–323. doi: 10.1007/s004240050785
37. Navedo MF, Amberg GC, Votaw VS, Santana LF. Constitutively active L-type Ca^{2+} channels. *Proc Natl Acad Sci USA*. 2005;102:11112–11117. doi: 10.1073/pnas.0500360102
38. Prada MP, Syed AU, Reddy GR, Martin-Aragon Baudel M, Flores-Tamez VA, Sasse KC, Ward SM, Sirish P, Chiamvimonvat N, Bartels P, et al. AKAP5 complex facilitates purinergic modulation of vascular L-type Ca(2+) channel CaV1.2. *Nat Commun*. 2020;11:5303. doi: 10.1038/s41467-020-18947-y
39. Chung SH, Kennedy RA. Coupled Markov chain model: characterization of membrane channel currents with multiple conductance sublevels

as partially coupled elementary pores. *Math Biosci*. 1996;133:111–137. doi: 10.1016/0025-5564(95)00084-4
40. Veatch SL, Machta BB, Shelby SA, Chiang EN, Holowka DA, Baird BA. Correlation functions quantify super-resolution images and estimate apparent clustering due to over-counting. *PLoS One*. 2012;7:e31457. doi: 10.1371/journal.pone.0031457
41. Sengupta P, Jovanovic-Talisman T, Skoko D, Renz M, Veatch SL, Lippincott-Schwartz J. Probing protein heterogeneity in the plasma membrane using PALM and pair correlation analysis. *Nat Methods*. 2011;8:969–975. doi: 10.1038/nmeth.1704
42. Amberg GC, Navedo MF, Nieves-Cintron M, Molkentin JD, Santana LF. Calcium sparklets regulate local and global calcium in murine arterial smooth muscle. *J Physiol*. 2007;579:187–201. doi: 10.1113/jphysiol.2006.124420
43. Amberg GC, Rossow CF, Navedo MF, Santana LF. NFATc3 regulates Kv2.1 expression in arterial smooth muscle. *J Biol Chem*. 2004;279:47326–47334. doi: 10.1074/jbc.M408789200
44. Nieves-Cintrón M, Amberg GC, Nichols CB, Molkentin JD, Santana LF. Activation of NFATc3 Down-regulates the β1 subunit of large conductance, calcium-activated K^+ channels in arterial smooth muscle and contributes to hypertension. *J Biol Chem*. 2007;282:3231–3240. doi: 10.1074/jbc.M608822200
45. Hayabuchi Y, Standen NB, Davies NW. Angiotensin II inhibits and alters kinetics of voltage-gated K^+ channels of rat arterial smooth muscle. *Am J Physiol Heart Circ Physiol*. 2001;281:H2480–H2489. doi: 10.1152/ajpheart.2001.281.6.H2480
46. Pires PW, Ko EA, Pritchard HAT, Rudokas M, Yamasaki E, Earley S. The angiotensin II receptor type 1b is the primary sensor of intraluminal pressure in cerebral artery smooth muscle cells. *J Physiol*. 2017;595:4735–4753. doi: 10.1113/JP274310
47. Jackson KL, Head GA, Gueguen C, Stevenson ER, Lim K, Marques FZ. Mechanisms responsible for genetic hypertension in Schlager BPH/2 mice. *Front Physiol*. 2019;10:1311. doi: 10.3389/fphys.2019.01311
48. Tajada S, Cidad P, Colinas O, Santana LF, Lopez-Lopez JR, Perez-Garcia MT. Down-regulation of CaV1.2 channels during hypertension: how fewer CaV1.2 channels allow more Ca(2+) into hypertensive arterial smooth muscle. *J Physiol*. 2013;591:6175–6191. doi: 10.1113/jphysiol.2013.265751
49. Nelson MT, Standen NB, Brayden JE, Worley JF III. Noradrenaline contracts arteries by activating voltage-dependent calcium channels. *Nature*. 1988;336:382–385. doi: 10.1038/336382a0
50. Sato D, Hernandez-Hernandez G, Matsumoto C, Tajada S, Moreno CM, Dixon RE, O'Dwyer S, Navedo MF, Trimmer JS, Clancy CE, et al. A stochastic model of ion channel cluster formation in the plasma membrane. *J Gen Physiol*. 2019;151:1116–1134. doi: 10.1085/jgp.201912327
51. Voelker TL, Del Villar SG, Westhoff M, Costa AD, Coleman AM, Hell JW, Horne MC, Dickson EJ, Dixon RE. Acute phosphatidylinositol 4,5 bisphosphate depletion destabilizes sarcolemmal expression of cardiac L-type Ca(2+) channel Ca(V)1.2. *Proc Natl Acad Sci USA*. 2023;120:e2221242120. doi: 10.1073/pnas.2221242120
52. Ghosh D, Nieves-Cintron M, Tajada S, Brust-Mascher I, Horne MC, Hell JW, Dixon RE, Santana LF, Navedo MF. Dynamic L-type CaV1.2 channel trafficking facilitates CaV1.2 clustering and cooperative gating. *Biochim Biophys Acta Mol Cell Res*. 2018;1865:1341–1355. doi: 10.1016/j.bbamcr.2018.06.013
53. Folci A, Steinberger A, Lee B, Stanika R, Scheruebel S, Campiglio M, Ramprecht C, Pelzmann B, Hell JW, Obermair GJ, et al. Molecular mimicking of C-terminal phosphorylation tunes the surface dynamics of CaV1.2 calcium channels in hippocampal neurons. *J Biol Chem*. 2018;293:1040–1053. doi: 10.1074/jbc.M117.799585
54. O'Dwyer SC, Palacio S, Matsumoto C, Guarina L, Klug NR, Tajada S, Rosati B, McKinnon D, Trimmer JS, Santana LF. Kv2.1 channels play opposing roles in regulating membrane potential, Ca(2+) channel function, and myogenic tone in arterial smooth muscle. *Proc Natl Acad Sci USA*. 2020;117:3858–3866. doi: 10.1073/pnas.1917879117
55. Matsumoto C, O'Dwyer SC, Manning D, Hernandez-Hernandez G, Rhana P, Fong Z, Sato D, Clancy CE, Vierra NC, Trimmer JS, et al. The formation of K(V)2.1 macro-clusters is required for sex-specific differences in L-type Ca(V)1.2 clustering and function in arterial myocytes. *Commun Biol*. 2023;6:1165. doi: 10.1038/s42003-023-05527-1
56. Xue B, Pamidimukkala J, Hay M. Sex differences in the development of angiotensin II-induced hypertension in conscious mice. *Am J Physiol Heart Circ Physiol*. 2005;288:H2177–H2184. doi: 10.1152/ajpheart.00969.2004
57. Connelly PJ, Currie G, Delles C. Sex differences in the prevalence, outcomes and management of hypertension. *Curr Hypertens Rep*. 2022;24:185–192. doi: 10.1007/s11906-022-01183-8